Simulation of Neurotransmitter Sensing by Cyclic Voltammetry under Mechanical Motion of a Neural Electrode

S. Han[1], M. Polanco[2], H. Yoon[1], S. Bawab[2]
[1] Department of Engineering, Norfolk State University, Norfolk, VA, USA
[2] Department of Mechanical and Aerospace Engineering, Old Dominion University, Norfolk, VA, USA

Abstract

The micromotion experienced by implanted neural probes within the brain can impact its capability to sense neurotransmitters. COMSOL Multiphysics is utilized to assess the degree of oxidation and reduction levels of neurochemicals from the motion incurred onto the probe. Various mechanical frequencies, different levels of adhesion, and voltammetry scan rates from the probe are assessed throughout time in measuring cyclic voltammetry of the neurochemicals. The results show that mechanical motion of the electrode greatly disturbs ionic transport through the brain tissue, particularly during peak values of oxidation and reduction. The results obtained here can be used to understand the effects of micromotion and astro-glial sheath formation on sensing signals and aiding chronic neurotransmitter sensing immune to the mechanical noises.

Introduction

Neural probes are embedded within the brain for sensing of electrophysical and neurochemical signals [1] or localized neuronal stimulation [2]. They are utilized either as a single entity [3] or a multi-channel array [4] in the brain. Designing neural probes to accurately detect chemicals within the brain for long periods of time has proven to be challenging due to micromotion, resulting from vascular pulsation, breathing, or external mechanical disturbances such as motion or impacts. It is estimated that the magnitude of displacement from internal disturbance ranges from 1-4 μm for pulsation to 25 μm for breathing [5]. The frequencies that have been measured are usually 1-2 Hz for breathing and 3-4 Hz for pulsation. When external impact is applied, the magnitude and frequencies can easily exceed the range depending on the type of mechanical impacts. Micromotion disturbances affect the sensing reliability of neural probes. It is considered micromotion of neural probe in the brain is one of major sources of neuronal tissue damages and astro-glial sheath formation by immune system response. This can occur as early as 2-4 weeks after a probe has been inserted into the brain [6]. The neuronal cell degeneration and sheath formation surrounding the neural electrodes hinder its ability to accurately sense electrophysiological and chemical activity within the brain.

Cyclic voltammetry assesses neurochemical activity produced by neurons and pertaining to kinetic reaction of neural transmitters [7,8]. Using a series of sweeping potentials, a neural probe or probes can sense in-vivo the transport of ions within the brain and thus identify their chemical kinetics. The practice has its benefits in assessing neurotransmitter imbalances in mental health patients. However, internal or external mechanical disturbances imparted upon the probe can cause irregularities in the in-vivo chemical sensing characteristics, leading to potential inaccuracies measuring the kinetics of ions.

Previous studies have examined the effect of stiffness discrepancy between various probe materials and adjacent brain tissue because of internal and external disturbances within the brain [9-10]. Damage to surrounding tissue from the probe was assessed because of different mechanical motion profiles as a function of frequency and displacement. Studies assessing chemical kinetics as a function of mechanical disturbances have been lacking. The present study is extended to include the effect of the ionic transport of neurotransmitters in the brain when mechanical disturbances are present using COMSOL Multiphysics.

The following study will focus on the mechanical-electrochemical coupling behaviors in neurochemical sensing using cyclic voltammetry including the diffusion of dopamine molecules within the brain tissue given its strong interest in neuroscience studies and clinical applications. Dopamine plays different roles as a neurotransmitter, including motor control, release of various hormones, and is primarily the driver in evoking positive behavior and emotions in humans. Its deficiency has also been linked to various mental disorders such as Parkinson's Disease and ADHD [11]. The diffusion of dopamine throughout the brain tissue around sensing electrodes is studied as mechanical disturbances are employed.

Simulation Methods

The following study utilizes both the Structural Mechanics and Electrochemistry modules to effectively capture the ionic diffusion of dopamine coupled with mechanical motion of the embedded neural probe. The study also seeks to establish viable modeling methods in accordance with physics to carry into future studies. In doing this, a two-dimensional Finite Element model was assumed.

The Structural Mechanics/Solid Mechanics module was used to model the material properties of the probe and the brain. The Solid Mechanics module is utilized primarily to prescribe mechanical motion of the probe onto the brain. The properties of each entity can be found in Table 1. A picture of the model can be found in Figure 1. The electrode utilized in the simulation contained parameters of an 8 µm length and a 2 µm width to model a carbon fiber electrode with a sharp tip exposed, while the size of the brain model was 52 µm by 48 µm in length and width respectively. Model dimensions were chosen to properly capture the ionic diffusion throughout the brain medium. As most of the diffusion was expected to take place along the electrode surface to brain interface, a mesh was concentrated within the vicinity of the probe.

Table 1. Material Properties

Material	Young's Modulus (Pa)	Poisson's Ratio	Density (kg/m^3)
Polyimide [12]	2.8 x 10^9	0.33	1330
Brain [13]	15000	0.45	1050

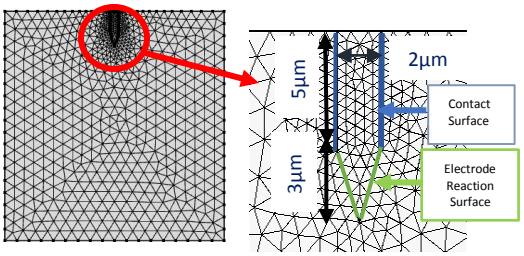

Figure 1. Finite Element Model

The brain was modeled using the Kelvin-Voigt viscoelastic material model in conjunction with the material properties shown in Table 1. A relaxation time of 12.5 ms was prescribed in accordance with the relaxation properties used in [9-10]. The linear elastic material model makes use of the linear elasticity equation of motion to govern deformation patterns within a body (Equation 1).

$$\rho \frac{\partial^2 \boldsymbol{u}}{\partial t^2} - \nabla \cdot \sigma = \boldsymbol{F}v$$

Equation 1. Linear Elasticity Equation of Motion

To represent the mechanical motion of the carbon fiber electrode, the prescribed displacement module was applied using a sinusoidal waveform, representing the internal or external disturbances imparted into the brain. An example of one of the waveforms used can be found in Figure 2. The displacement was applied on the top boundary of the probe onto the brain while the boundaries of the brain were fixed in all degrees of freedom. Three different frequency values were examined: 0, 0.1, and 1 Hz., in this study to represent just the internal micromotion inside the brain with a displacement magnitude of 1 µm. The use of contact via penalty method was utilized to simulate different stages of bonding between the probe and the brain resulting from potential sheath formation during the implantation period. Bonding was established in the model by employing different coefficients of friction (mu) : 0, to represent initial insertion, and 0.1, 0.3, and 1 to represent different stages of bonding along the probe to brain interface. The higher the coefficient, the higher the degree of bonding between the probe and brain interface.

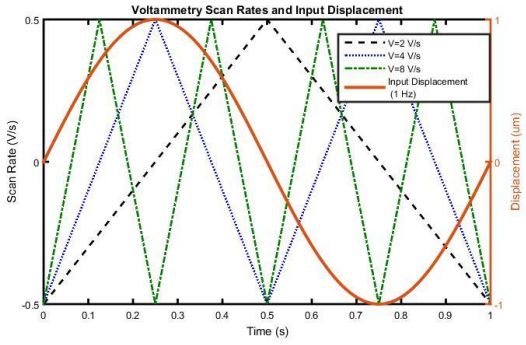

Figure 2. Voltammetry Scan Rates and Prescribed Sinusoidal Displacement for Slow Scan Rate

To represent the diffusion of dopamine, the electrochemistry module was employed. Cyclic voltammetry was used to employ various scan rates in conjunction with the prescribed mechanical motion. The source of the voltage sweep was applied

at the tip of the embedded probe, while the sink was applied at the modeled boundaries of the brain. Slow Scan rates of 2, 4, and 8 V/s were utilized for this model with a range between -0.5 and 0.5 V, as shown in Figure 2. The chemical kinetics utilized Equations 2 and 3 to simulate diffusion within the brain during cyclic voltammetry. The standard homogeneous constant k_0 was set to 0.01 m/s.

The double layer capacitance feature in Equation 4 was introduced into the model to represent different degrees of energy being both stored and discharged during the voltammetry cycle. A capacitance value of 0.1 F/m^2 was used in all cases, while the governing equation used is represented by Equation 4. All cases were run for 1 second.

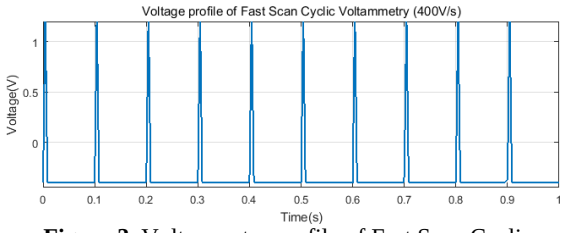

Figure 3. Voltammetry profile of Fast Scan Cyclic Voltammetry

In experimental dopamine sensing, fast scan cyclic voltammetry (FSCV) is normally utilized. To simulate realistic FSCV, the voltage trace in Figure 3 was applied. The graph shows a 400V/s scan rate with 100ms resting duration between peaks was applied with a range between -0.4 and 1.2V, which is normally used for FSCV for dopamine sensing. To represent mechanical motion, 1Hz sinusoidal waveform was also used with two different double layer capacitance 0.01F/ m^2 and 0.1F/ m^2.

$$\frac{\partial c_i}{\partial t} + \nabla \cdot (-D_i \nabla c_i) = R_i\,, \quad R_i = \frac{v_i i_{loc}}{nF}$$

Equation 2. Nernst-Planck equation

$$i_{loc} = nFk_0\left(c_{red} exp\frac{(n-\alpha_C)F\eta}{RT} - c_{ox} exp\frac{(-\alpha_C)F\eta}{RT}\right)$$
$$(\eta = \phi_{s,\,ext} - E_{eq})$$

Equation 3. Butler-Volmer equation

$$i_{dl} = (\frac{\partial \phi_s}{\partial t})C_{dl}$$

Equation 4. Double layer capacitance

Results

Simulating Cyclic Voltammetry under micro motion utilizes two different modules. It was successful to capture electro-mechanical coupling using the structural and electroanalysis modules. The voltammetry plots show considerable differences in chemical kinetics when motion of the probe is employed and when the probe is stationary. Figures 3a-3c show redox characteristics of brain chemical during the voltammetry process when the probe moves under a mechanical frequency of 1Hz depending on bonding conditions between the probe and brain tissue. Higher scan rates show that the magnitudes of current density become more disparate when dopamine has reached both its peak reduction and oxidation potentials. In addition, higher scan rates allow for higher transfer of ions throughout the brain. However, when the probe becomes increasingly bonded to the brain at its interface, the peak current density magnitudes drop. Table 2 shows the approximate drop in current density magnitude between no bonding and maximum bonding. Only the cases for 1 Hz is shown as no visible differences in the redox reaction were noted. All cases show the voltammetry graphs when the first cycle was applied in the model.

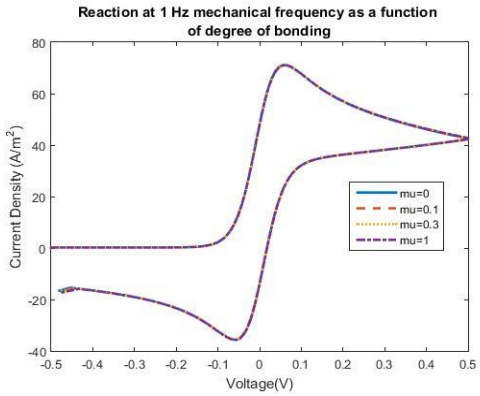

(a) Scan rate = 2 V/s

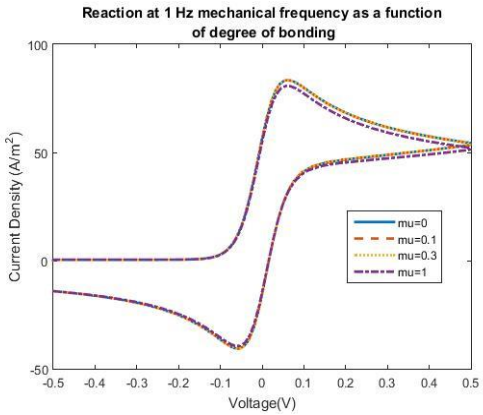

(b) Scan rate = 4 V/s

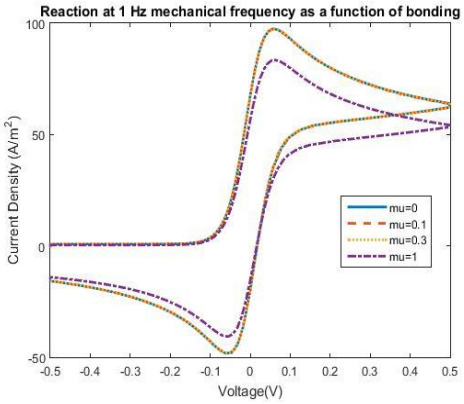

(c) Scan rate = 8 V/s

Figure 4. Redox reaction characteristics as a function of voltammetry scan rate and friction coefficient

Table 2. Differences in Peak Current Magnitudes between no bonding and maximum bonding

Scan Rate	Current Density
2 V/s	0 A/m^2
4 V/s	2.5 A/m^2
8 V/s	14 A/m^2

As shown in Figure 5, no visible differences are seen in the cyclic voltammetry graphs when mechanical frequency is varied under no applied friction between the probe and the brain. However, an increase in the current density magnitudes is visible as the scan rate increases. As with varying friction coefficients, increasing the scan rate also increases the magnitude of the current density. In Figure 6, when maximum bonding is activated, the current density magnitude is shown to decrease compared to cases when the probe is considered stationary. Table 3 highlights the differences in peak magnitudes between a stationary and moving probe.

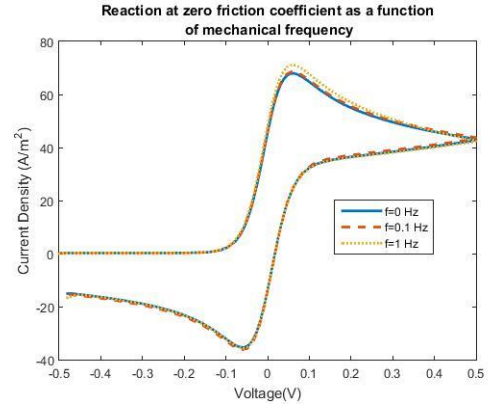

(a) Scan rate = 2 V/s

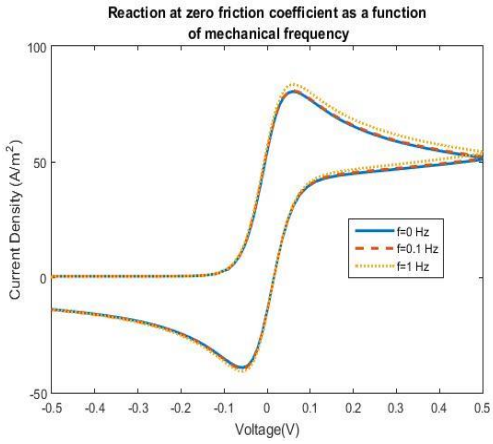

(b) Scan rate = 4 V/s

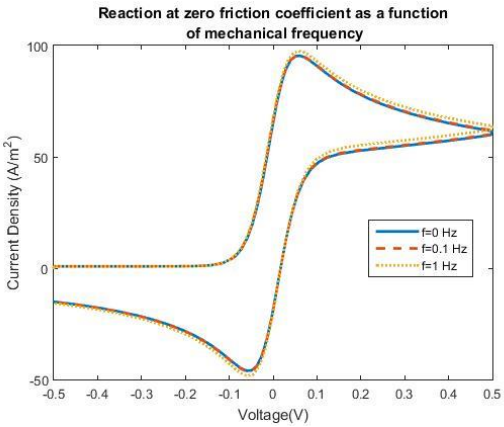

(c) Scan rate = 8 V/s

Figure 5. Redox reaction of dopamine as a function of mechanical frequency under no friction

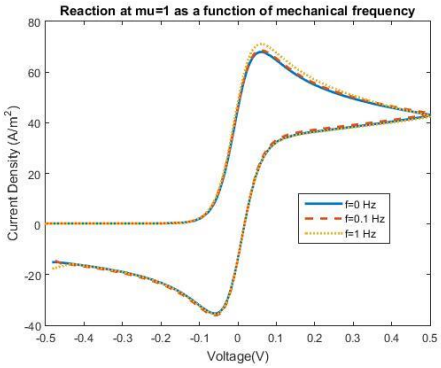

(a) Scan rate = 2 V/s

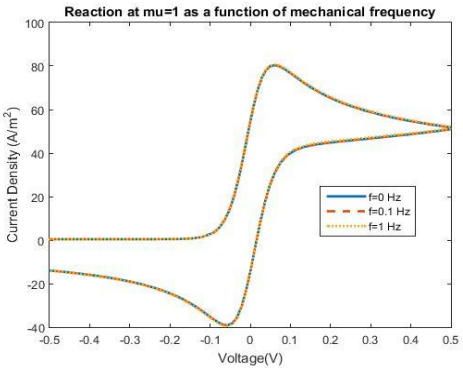

(b) Scan rate = 4 V/s

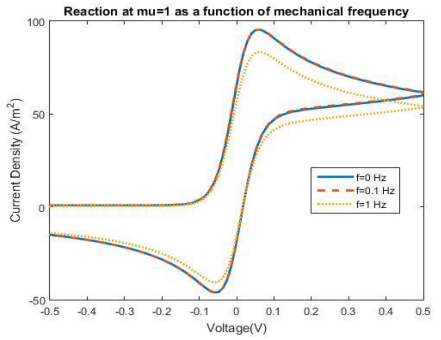

(c) Scan rate = 8 V/s

Figure 6. Redox reaction of dopamine as a function of mechanical frequency under maximum bonding

Table 3. Differences in Peak Current Magnitudes during maximum bonding between a stationary and moving probe (1 Hz)

Scan Rate	Current Density
2 V/s	3.2 A/m^2
4 V/s	0.8 A/m^2
8 V/s	-12 A/m^2

Image results using FSCV in Figure 7 shows the simulation results using FSCV at one simulated time point during the 1s time interval. For fast scan cyclic voltammetry, the third cycle is represented in Figure 8 among 10 cycles of scanning for 1s.

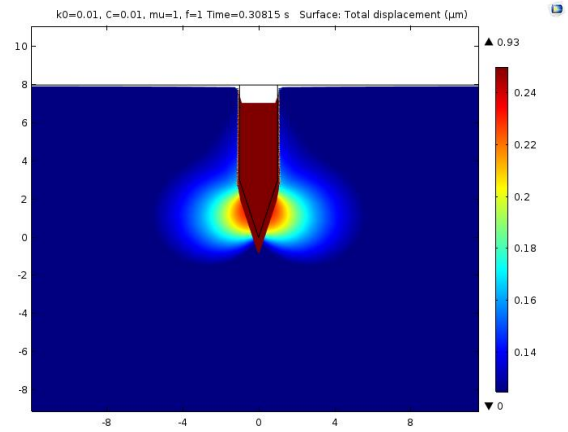

(a) Displacement

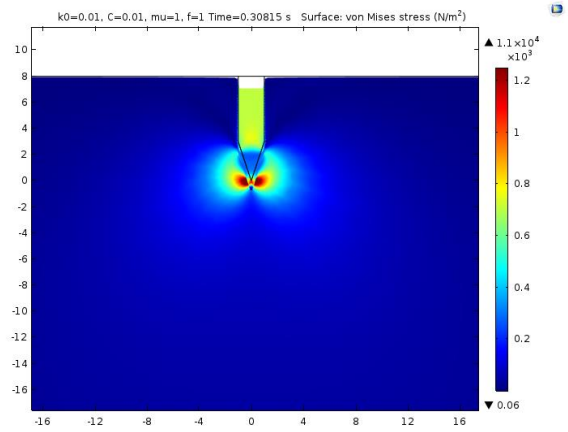

(b) Von Mises stress

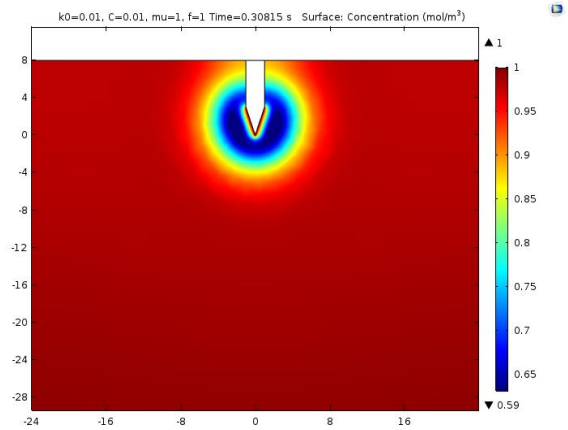

(c) Concentration of oxidized species

Figure 7. 2D plots representing results of Cyclic Voltammetry (400V/s) under 1Hz mechanical motion.

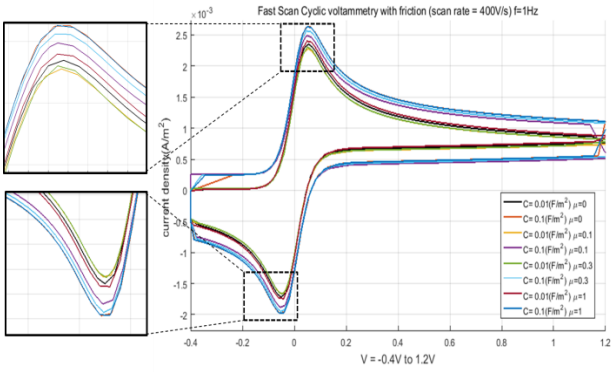

Figure 8. Redox reaction of dopamine by FSCV under varied mechanical bonding and frequency, and double layer capacitance.

Table 4. Differences in Peak Current Magnitudes between a stationary and moving probe (1 Hz) during oxidation in Fast Scan Cyclic Voltammetry

Double Layer Capacitance	Mechanical friction Coefficient	Current Density Difference
0.01F/ m^2	0	80.7 µA/m^2
0.1F/ m^2	0	149 µA/m^2
0.01F/ m^2	0.1	20.0 µA/m^2
0.1F/ m^2	0.1	58.7 µA/m^2
0.01F/ m^2	0.3	39.0 µA/m^2
0.1F/ m^2	0.3	80.9 µA/m^2
0.01F/ m^2	1	140 µA/m^2
0.1F/ m^2	1	145 µA/m^2

Table 5. Differences in Peak Current Magnitudes between a stationary and moving probe (1 Hz) during reduction in Fast Scan Cyclic Voltammetry

Double Layer Capacitance	Mechanical friction Coefficient	Current Density Difference
0.01F/ m^2	0	-53.2 µA/m^2
0.1F/ m^2	0	-107 µA/m^2
0.01F/ m^2	0.1	-22.4 µA/m^2
0.1F/ m^2	0.1	-64.7 µA/m^2
0.01F/ m^2	0.3	-72.0 µA/m^2
0.1F/ m^2	0.3	-70.2 µA/m^2
0.01F/ m^2	1	-110 µA/m^2
0.1F/ m^2	1	-115 µA/m^2

In case of FSCV, current density difference also becomes large when the mechanical friction gets higher. Regarding double layer, increased capacitance makes high current density difference, but the effect of capacitance tends to decrease when high mechanical friction coefficient is introduced. In Table 4 and Table 5, current density differences of two different capacitance values shows similar large values when maximum bonding is introduced. In case of no bonding, current density is highly affected by double layer capacitance.

Discussion

The purpose of this study was to assess the chemical kinetics of dopamine using cyclic voltammetry under micromotion of the brain. To our knowledge, this type of coupling has not been investigated in aiding the design of -chronic neural probes.

Based on this study, key findings were made with the redox reactions that were measured in the simulation. To be able to detect neurotransmitters in the brain accurately, the scan rate in cyclic voltammetry becomes important to consider as the scan rate is the factor of obtaining kinetic information of brain chemical. As the degree of bonding increases over time between the probe and the brain, and as the rate of mechanical motion increases, redox characteristics are shown to be altered compared to initial insertion of the probe or stationary position. In addition, when the probe can move more freely, the redox reactions do not show any variance with respect to applied voltage.

This preliminary study has established a viable model methodology in moving forward with future research. A 3D model of the probe and the brain will be constructed while employing voltage scans from an embedded probe associated with fast scan cyclic voltammetry. This will employ multiple scan cycles to assess long term characteristics of dopamine and other neurotransmitters over time. In addition, higher frequencies and magnitudes associated with micromotion and external motion will be applied. It is expected that the redox reactions of dopamine will differ greatly when additional parameters are introduced in this study.

Conclusion

A study investigating the chemical kinetics of dopamine with respect to mechanical motion imparted by the brain was conducted. Mechanical frequencies up to 1 Hz and various bonding coefficients were introduced as parameter values in

the model. The results show that the chemical kinetics can be altered greatly when the probe deviates from a stationary position, or becomes more bonded to surrounding neurons. Thus, it becomes important to consider how voltammetry scan rates are applied within the brain to detect the presence of various neurotransmitters. The study provides a first step in a building block approach towards understanding the implications in the brain's micromotion disturbance and analyzing neurochemical sensing signals depending on the condition of astro-glial sheath formation.

References

[1] M.D. Johnson, J.C. Williams, M. Holecko, D.R. Kipke. "Chemical sensing capability of MEMS implantable multichannel arrays," in *Proc. 25th Annual International Conference of IEEE EMBS*, (2003).

[2] S. Takeuchi, T. Suzuki, K. Mabuchi, H. Fujita. "3D flexible multichannel neural probe array." *Micromechanics and Microengineering*," **14**, Issue 1, (2003).

[3] J. Subbaroyan, D.C. Martin, D.R. Kipke "A finite-element model of the mechanical effects of implantable microelectrodes in the cerebral cortex," *Journal of Neural Engineering*, **2**, pp.103-113, (2005).

[4] A. Lavacchi, U. Bardi, C. Borri, S. Caporali, A. Fossati, I. Perissi, "Cyclic voltammetry simulation at microelectrode arrays with COMSOL Multiphysics^{TM} " *Applied Electrochemistry***, 39**, pp. 2159-2163, (2009).

[5] J. Muthuswamy, A. Gilletti, T. Jain, and M. Okandan. "Microactuated Neural Probes to Compensate for Brain Micromotion," in *Proc. 25th Annual International Conference of IEEE EMBS 2*, pp. 1941-1943, (2003).

[6] J.N. Turner, W. Shain, D.H. Szarowski, M. Anderson, S. Martins, M. Isaacson; H.G. Craighead. "Cerebral astrolyte response to micromachined silicon implants," *Experimental Neurology*, **156**, pp. 33-49, (1999).

[7] J.C. Patel. *Voltammetry: Electrochemical Detection of Neurotransmitters in the Brain.* S. John Wiley & Sons Ltd, Chichester, (2016).

[8] A.J. Bard., L.R. Faulkner. *Electrochemical Methods: Fundamentals and Applications.* Wiley, New York, (2001).

[9] M. Polanco, H. Yoon, S. Bawab. "Micromotion-induced Dynamic Effects from a Neural Probe and Brain Tissue Interface," *Micro/Nanolithography, MEMS, and MOEMS*, **13**, Issue 2, (2014).

[10] M. Polanco, H. Yoon, and S. Bawab. "Computational Assessment of Neural Probe and Brain Tissue Interface under Transient Motion," Journal of *Biosensors*, **6**, Issue 2, (2016).

[11] N.D. Volkow, G.J. Wang, S.H. Kollins, T.L. Wigal, J.H. Newcorn, F. Telang, J.S. Fowler, W. Zhu, J. Logan, Y. Ma, K. Pradhan, C. Wong, J.M. Swanson. "Evaluating dopamine reward pathway in ADHD: clinical implications," *JAMA*., **302**, Issue 10, pp. 1084–1091, (2009).

[12] A. Mercanzini, K. Cheung, D. Buhl, M. Boers, A. Maillard, P. Colin, J. Bensadoun, A. Bertsch, A. Carleton, P. Renaud. "Determination of cortical recording and reduced inflammatory response using flexible polymer neural probes," in *Proceedings of the IEEE MEMS Conference Kobe (Japan*), (2007).

[13] H. Lee, R.V. Bellamkonda, W. Sun, and M.E. Levenston. "Biomechanical analysis of silicon microelectrode-induced strain in the brain," *Neural Engineering*, **2**, pp. 81-89, (2005).

Appendix

Nomenclature

ρ – mass density

∇ – del operator

σ – Cauchy Stress Tensor

ν – Poisson's ratio

μ – Friction Coefficient

D_i – Diffusion coefficient

F – Faraday's Constant

n – number of electrons involved in reaction

k_0 – Boltzmann Constant

c_{red} – Reduction species concentration

c_{ox} – Oxidation species concentration

R – Universal gas constant

T- Temperature

η – Activation overpotential

α_C – Cathode transfer potential

$\phi_{s,ext}$ – Electrode potential

E_{eq} – Equilibrium potential

i_{dl} – Double layer current

ϕ_s – Capacitance voltage

C_{dl} – Double layer capacitance